An ab Initio Molecular Dynamics Study of the Aqueous Liquid-Vapor Interface

I-Feng W. Kuo and Christopher J. Mundy

Science **303**, 658 (2004);
DOI: 10.1126/science.1092787

Science (print ISSN 0036-8075; online ISSN 1095-9203) is published weekly, except the last week in December, by the American Association for the Advancement of Science, 1200 New York Avenue NW, Washington, DC 20005.

3. S. J. Tans *et al.*, *Nature* **386**, 474 (1997).
4. M. Bockrath *et al.*, *Science* **275**, 1922 (1997).
5. J. Kong, C. W. Zhou, E. Yenilmez, H. J. Dai, *Appl. Phys. Lett.* **77**, 3977 (2000).
6. D. Loss, D. P. DiVincenzo, *Phys. Rev. A.* **57**, 120 (1998).
7. D. P. DiVincenzo, D. Bacon, J. Kempe, G. Burkard, K. B. Whaley, *Nature* **408**, 339 (2000).
8. Multiple quantum dots without independent control have been observed previously in carbon nanotubes. See (*10*) and (*11*).
9. K. Ishibashi, M. Suzuki, T. Ida, Y. Aoyagi, *Appl. Phys. Lett.* **79**, 1864 (2001).
10. J. Lefebvre, J. F. Lynch, M. Llaguno, M. Radosavljevic, A. T. Johnson, *Appl. Phys. Lett.* **75**, 3014 (1999).
11. M. J. Biercuk, N. Mason, C. M. Marcus, *Nano Lett.*, in press, published online 19 November 2003.
12. S. J. Wind, J. Appenzeller, P. Avouris, *Appl. Phys. Lett.* **80**, 3817 (2002).
13. Materials and methods are available as supporting material on *Science* Online.
14. Measurements of conductance as a function of bias voltage and gate voltage show Coulomb blockade with two nearly equivalent charging energies, indicating that the two dots are of equal size. The symmetry of the honeycombs in Fig. 2 also indicates that the charging energies of the two dots are nearly equal.
15. M. Bockrath *et al.*, *Science* **291**, 283 (2001).
16. L. Chico, L. X. Benedict, S. G. Louie, M. L. Cohen, *Phys. Rev. B* **54**, 2600 (1996).
17. T. Kostyrko, M. Bartkowiak, G. D. Mahan, *Phys. Rev. B* **59**, 3241 (1999).
18. H. J. Choi, J. Ihm, S. G. Louis, M. L. Cohen, *Phys. Rev. Lett.* **84**, 2917 (2000).
19. M. J. Biercuk, N. Mason, J. Chow, C. M. Marcus, available at http://arXiv.org/abs/cond-mat/0312276.
20. W. G. van der Wiel *et al.*, *Rev. Mod. Phys.* **75**,1 (2003).
21. N. C. van der Vaart *et al.*, *Phys. Rev. Lett.* **74**, 4702 (1995).
22. T. Fujisawa *et al.*, *Science* **282**, 932 (1998).
23. D. V. Averin Yu, V. Nazarov, in *Single Charge Tunneling: Coulomb Blockade Phenomena in Nanostructures*, H. Grabert, M. H. Devoret, Eds. (Plenum Press and NATO Scientific Affairs Division, New York/London, 1992).
24. J. Hone, B. Batlogg, Z. Benes, A. T. Johnson, J. E. Fischer, *Science* **289**, 1730 (2000).
25. J. Vavro *et al.*, *Phys. Rev. Lett.* **90**, 65503 (2003).
26. C. Livermore, C. H. Crouch, R. M. Westervelt, K. L. Campman, A. C. Gossard, *Science* **274**, 1332 (1996).
27. L. P. Kouwenhoven *et al.*, in *Mesoscopic Electron Transport*, L. P. Kouwenhoven, G. Schön, L. L. Sohn, Eds. (Kluwer, Dordrecht, Netherlands, 1997).
28. A. Kaminksi, L. I. Glazman, *Phys. Rev. B* **59**, 9798 (1999).
29. K. A. Matveev, L. I. Glazman, H. U. Baranger, *Phys. Rev. B* **54**, 5637 (1996).
30. 1/T behavior is expected for $\Gamma < k_B T \ll \Delta$.

31. The authors wish to thank J. Hone, A. C. Johnson, and J. B. Miller for useful discussions, and H. Park for assistance with the design of the nanotube chemical vapor deposition system. This work was supported by funding from the NSF through the Harvard Materials Research Science and Engineering Center, the NSF under EIA-0210737, and the Army Research Office/Advanced Research and Development Authority Quantum Computing Program. N.M. acknowledges support from the Harvard Society of Fellows. M.J.B. acknowledges support from an NSF Graduate Research Fellowship and from an ARO Quantum Computing Graduate Research Fellowship.

Supporting Online Material

www.sciencemag.org/cgi/content/full/303/5658/655/DC1

Materials and Methods

13 November 2003; accepted 24 December 2003

An ab Initio Molecular Dynamics Study of the Aqueous Liquid-Vapor Interface

I-Feng W. Kuo and Christopher J. Mundy*

We present an ab initio molecular dynamics simulation of the aqueous liquid-vapor interface. Having successfully stabilized a region of bulk water in the center of a water slab, we were able to reproduce and further quantify the experimentally observed abundance of surface "acceptor-only" (19%) and "single-donor" (66%) moieties as well as substantial surface relaxation approaching the liquid-vapor interface. Examination of the orientational dynamics points to a faster relaxation in the interfacial region. Furthermore, the average value of the dipole decreases and the average value of the highest occupied molecular orbital for each water molecule increases approaching the liquid-vapor interface. Our results support the idea that the surface contains, on average, far more reactive states than the bulk.

Although the nature of bulk liquid water itself remains incompletely understood, there is a more pressing need to characterize water in more complex environments. In particular, the interfaces between liquid water and hydrophobic material or air engender important phenomena in biology (*1*–*5*) and atmospheric science (*6*, *7*), respectively. These two interfaces seem to have much in common (*1*), and both are currently the subject of intense scrutiny.

Experimentalists have led the way in characterizing the aqueous liquid-vapor interface. Measurements of the aqueous liquid-vapor interface have provided proof of dangling OH bonds present at the surface (*8*, *9*). Recent x-ray experiments on the aqueous liquid-vapor interface have provided strong evidence for surface relaxation (*10*) and for new structural moieties in which both hydrogens (called "acceptor-only") of a surface water molecule are dangling (*11*, *12*). To date, theoretical models have not captured all these surface phenomena, presumably because the models were fitted to reproduce properties of the homogeneous bulk phases. Ab initio simulations lend themselves well to these studies because they present an unbiased representation of water in different environments and are thus ideal candidates for elucidating surface phenomena. Here, we used Car-Parrinello molecular dynamics (CPMD) (*13*, *14*) to investigate the properties of the aqueous liquid-vapor interface (*15*, *16*).

The shortest distance from the aqueous liquid-vapor interface at which one can observe bulk liquid behavior is ~10 Å (*17*). Due to the computational demands of ab initio methods, we needed to determine the smallest system one can simulate that will produce a stable interface. A recent ab initio study of the aqueous liquid-vapor interface using 32 waters produced interesting results regarding dangling bonds but

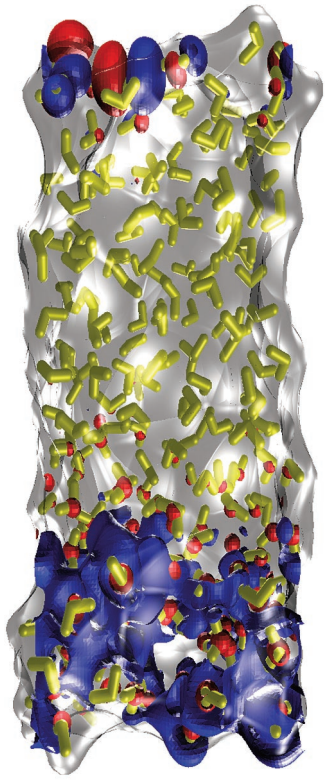

Fig. 1. Snapshot of the calculated aqueous liquid-vapor interface. The individual water monomers are represented by yellow cylinders. The colored isosurfaces on the top represent the HOMO, whereas the colored isosurfaces at the bottom represent the LUMO. The orbitals are obtained by direct diagonalization of the KS matrix, indicating that the reactivity of the water slab is localized on the surface for protons and electrons.

Computational Chemical Biology, Chemistry and Materials Science L-091, Lawrence Livermore National Laboratory, Livermore, CA 94550, USA.

*To whom correspondence should be addressed. E-mail: mundy2@llnl.gov

failed to stabilize a true interfacial system (*18*). The distance between the two free interfaces in that simulation was ~10 Å, well short of the ~30 Å needed to ensure a stable interfacial system (*17*).

Our ab initio simulation of the aqueous liquid-vapor interface (Fig. 1) was performed on 216 waters in a simulation cell of dimension 15 Å by 15 Å by 71.44 Å. The distance between the two free interfaces in the *z* direction was approximately 35 Å, indicating that there should be roughly 5 to 10 Å of bulk water. The initial configuration was obtained from classical molecular dynamics after an equilibration period of 100 ps at 300 K. After the initial wave function optimization, CPMD was performed for 4.9 ps (*19*).

A converged density profile is a true indicator of a stable interfacial system. Figure 2A depicts the density as a function of the slab coordinate *z*. We also report an analysis of each water based on the Voronoi polyhedron (*20*, *21*), which allows for the calculation of the average volume of a water molecule as a function of *z* (Fig. 2B). The analyses presented in Fig. 2 point conclusively to a region in the interior of the slab where water remains at bulk density. We have not constrained the bulk density to be 1 g/cm^3. Rather, we have allowed the system to come to its natural density based on our choice of pseudopotentials and exchange correlation functionals (*19*).

The robustness of our calculated interfacial properties depends on the existence of a finite region of bulk fluid in the center of the water slab. We verified the existence of bulk water both structurally and dynamically through the calculation of the radial distribution function (RDF), power spectrum, and rotational relaxation. Comparison of the RDF for bulk water and of the interior of the water slab (Fig. 3A) demonstrates that the structural properties of the interior region of the slab are representative of bulk water (*22*, *23*).

Sum frequency generation (SFG) experiments have been used to study the structure of the aqueous liquid-vapor interface (*8*, *9*). Experiments revealed two important features in the mid-infrared (IR) region. The first is a shoulder (~3250 cm^{-1}) of the broad peak at 3400 cm^{-1} attributed to the different hydrogen bond arrangements present at the interface (*8*, *9*, *24*). The second is a peak at ~3700 cm^{-1} assigned to an unperturbed OH vibration (*8*, *9*, *24*), which can be seen in our power spectrum (Fig. 3B). Due to our short trajectory, we cannot resolve the experimentally observed shoulder at ~3250 cm^{-1} (*24*). However, we did find hydrogen bonding arrangements at the interface that are distinct from the bulk liquid (Table 1) (*25*–*27*).

Recent x-ray absorption fine structure (NEXAFS) studies of liquid microjets carried out at the Lawrence Berkeley National Laboratory Advanced Light Source have provided the first evidence for a "acceptor-only" surface moiety (*12*) wherein both hydrogens of a surface water extend out of the liquid. This is different from the well-recognized "single donor" from which only one hydrogen dangles (*8*). Our power spectrum of the interfacial system does not allow us to discern between "single-donor" or "acceptor-only" configurations. However, using recent experimental work based on measurements of the proton magnetic shielding tensor to characterize the hydrogen bond geometry of liquid water as a function of temperature (*28*), it is now possible to use a hydrogen bond definition based on thermal population. For the hydrogen bond analysis, we define the length of a hydrogen bond as 1.59 to 2.27 Å for the oxygen-hydrogen separation and

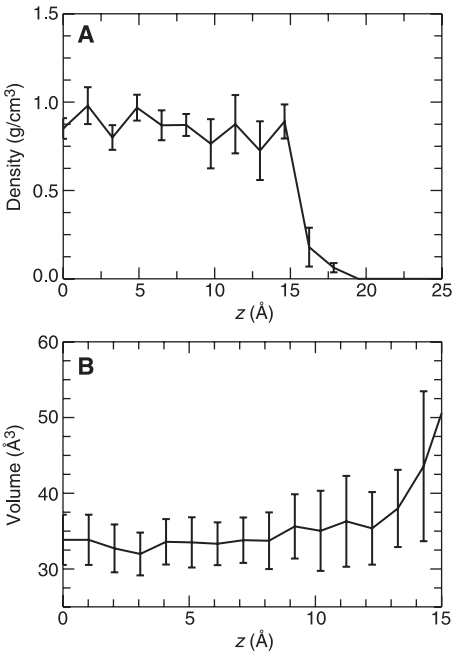

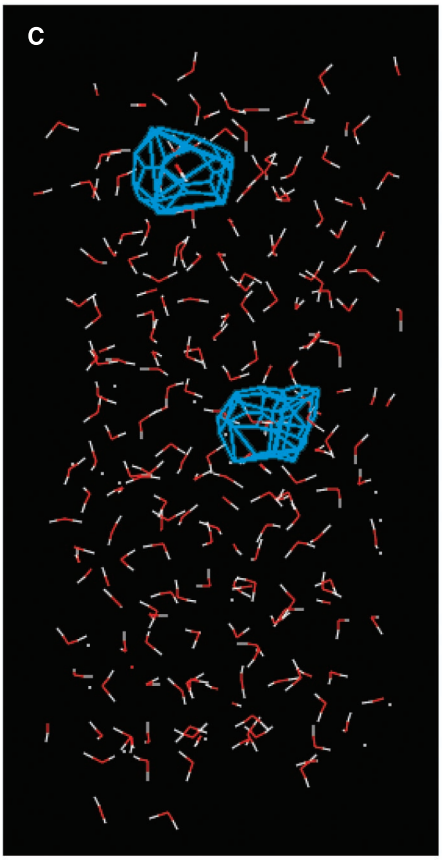

Fig. 2. (**A**) The density profile and (**B**) the volume per water molecule computed by the generation of Voronoi polyhedra, averaged over both interfaces, is plotted as a function of slab thickness *z*. Liquid water at ambient conditions has an average volume per water of 29.9 Å^3. Both panels indicate the presence of a stable interface; the error bars are standard deviations of the whole population. The Voronoi polyhedra reveal the experimentally observed surface relaxation (*10*, *11*) on approach toward the surface of the slab. The increase in the Voronoi volume occurs before the visually inferred Gibbs dividing surface of ~15 Å in (A). (**C**) A representative snapshot of a typical Voronoi polyhedra (blue) of a water molecule at both the interior and near the interface of the water slab. The polyhedron near the surface of the slab is not distorted, thus indicating that the observed volume expansion is not an artifact of the Voronoi analysis.

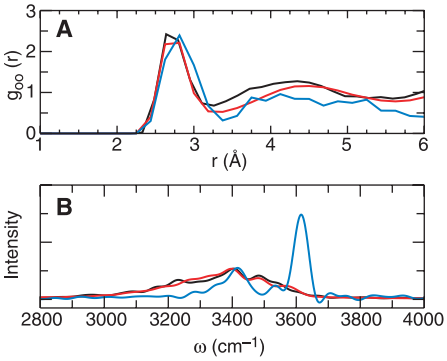

Fig. 3. (**A**) The oxygen-oxygen RDF and (**B**) power spectrum obtained from a bulk liquid water simulation (black), the interior of the slab (red), and the topmost 8 Å of the slab (blue). The bulk liquid water simulations were performed with CPMD on 64 waters at fixed volume corresponding to a density of 1 g/cm^3 for 11 ps, starting from a well-equilibrated configuration. The simulation parameters are identical to those of our slab system. (A) The interior region of the slab and the liquid water have identical first solvation shells. The second solvation shell of the interior region of the slab is slightly different from that of the bulk water simulation, probably because the density is not constrained in our slab simulation (Fig. 2). A slight expansion of the first solvation shell can be discerned in the RDF for the interfacial region, corroborating the observations of Wilson *et. al.* (*10*, *11*). (B) The mid-IR power spectrum as obtained from the Fourier transform of the total velocity autocorrelation function. For the bulk-like regions, a broad peak at 3400 cm^{-1} results from the red-shift of the OH vibration due to the presence of hydrogen bonds. For the surface of the slab, two peaks resolve; the second peak at 3625 cm^{-1} corresponds to an unperturbed OH vibration.

an angle greater than 140° between the reference oxygen and neighboring hydrogen and oxygen, respectively. These parameters were chosen to sample the experimentally determined hydrogen bond population within 4σ of the distance distribution at 300 K (*28*). With these criteria, we calculated for each individual water the number of hydrogen bonds partitioned into "acceptors" or "donors." For each hydrogen bond involving two waters, the reference oxygen involved in the hydrogen bond is considered the acceptor, whereas the neighboring water's hydrogen involved in the same hydrogen bond is considered the donor. Our results (Table 1) indicate that both single-donor and acceptor-only species are abundant, as proposed by the experiments of Wilson *et. al.* (*12*).

Recent extended x-ray absorption fine structure (EXAFS) experiments have also revealed a new picture of the aqueous liquid-vapor interface (*10*, *11*), characterizing a surface relaxation which is embodied as a reduced density near the interface. Ab initio techniques are well suited for the analysis of surface relaxation because of the natural incorporation of many-body polarization effects. Wilson *et. al.* (*10*, *11*) found a surface relaxation as a consequence of a 6% observed expansion of the oxygen-oxygen nearest neighbor distance in the vicinity of the interface. We also observed a slight increase in the oxygen-oxygen distance at the surface of the water slab (Fig. 3A). Furthermore, we saw a gradual rise in the average volume per water molecule as the interface is approached (Fig. 2B) as an additional signature of the experimentally observed surface relaxation.

The dynamical consequences of the different structure near the surface of our slab are evident both in the power spectrum (Fig. 3B) and in the rotational autocorrelation function (fig. S1). The faster relaxation and different librational dynamics occurring at the surface of the slab (*26*, *29*) can be attributed to the unsatisfied hydrogen bonding at the liquid-vapor interface suggested by Table 1.

In addition to structural and dynamical properties, ab initio simulations also reveal electronic properties that are not easily accessible via experiment and, thus, can be used as a predictive tool (*19*). To obtain a clear understanding of the electronic states involved in any potential chemistry, we transformed the Kohn-Sham (KS) states into the more intuitive molecular states (*30*). Thus, for each water molecule, we obtained four valence states resembling states with symmetry labels $1A_2$, $1B_2$, $2A_1$, and $1B_1$ of the isolated H_2O molecule (*30*). To gain further insight into the chemistry, we plotted the highest occupied molecular orbital (HOMO) (e.g., $1B_1$) of each molecule as a function of *z* (Fig. 4A). The states with highest energy, which are most likely to be involved in chemical reactions, are clearly located at the surface of our slab. We also made use of the Wannier Centroids (*31*) to approximate the individual dipole moment of water (Fig. 4B). The dipole moment dropped upon approach to the surface of the slab, indicating that polarization effects are indeed important. However, it remains to be seen how neglecting the polarization of water, as is done in the commonly with the use of fixed-charge models, will affect the calculated properties described here. Finally, the location of the HOMO and the lowest unoccupied molecular orbital (LUMO) (Fig. 1) for the water slab demonstrate that the surface of the slab is reactive to excess protons and electrons.

Table 1. The percentage of water molecules in a state as defined by its number of acceptor and donor hydrogen bonds averaged over the last 4 ps (*19*). The elements in each entry represent data obtained from a CPMD bulk liquid water simulation of 64 molecules, the interior region of the water slab, and the surface (5 Å in depth) of the water slab (colored black, red, and blue, respectively, in Fig. 3). Single-donor states have a substantial contribution (66%) to the total population at the surface as seen by summing the column with 1 hydrogen bond donor. Acceptor-only states are evident in the column with 0 hydrogen bond donors and also contribute substantially (19%), as proposed by Wilson *et. al* (*12*). The results presented here can also be mapped to recent work characterizing the spontaneous fluctuations of hydrogen bonded species in bulk water (SOM text).

No. of bond acceptors	No. of bond donors		
	0	1	2
0			
Bulk	2%	7%	3%
Interior	4%	9%	5%
Surface	5%	17%	1%
1			
Bulk	7%	24%	17%
Interior	5%	20%	13%
Surface	11%	36%	9%
2			
Bulk	3%	14%	20%
Interior	4%	16%	23%
Surface	3%	13%	4%

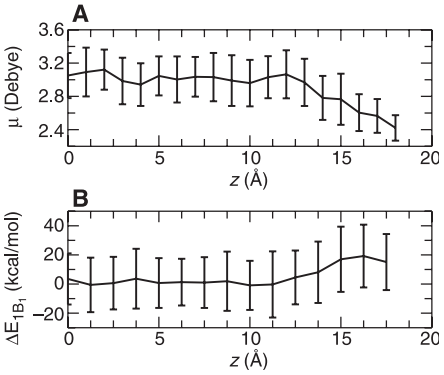

Fig. 4. The relative shift in the $1B_1$ molecular state (e.g., the HOMO) for each (**A**) dipole moment and (**B**) water, averaged over both interfaces, is plotted as a function of *z*. Error bars are determined by the standard deviation of the whole population. One can interpret (A) as the average change in the energy level of the HOMO of water molecule relative to that defined in the interior of the slab. Thus, there is a gain of ~10 to 15 kcal/mol near the liquid-vapor interface, suggesting the presence of a substantially more reactive surface. (A) In our simulations water deviates from its predicted bulk liquid dipole moment (*22*) of ~3.0 to ~2.4 Debye as one approaches the liquid-vapor interface. This points to weaker hydrogen bonds in the vicinity of the liquid-vapor interface.

References and Notes

1. P. Ball, *Nature* **423**, 25 (2003).
2. V. Yaminsky, S. Ohnishi, *Langmuir* **19**, 1970 (2003).
3. R. Steitz *et al.*, *Langmuir* **19**, 2409 (2003).
4. T. R. Jensen *et al.*, *Phys. Rev. Lett.* **90**, 086101 (2003).
5. K. Lum, D. Chandler, J. D. Weeks, *J. Phys. Chem. B* **103**, 4570 (1999).
6. M. S. Jang, N. M. Czoschke, S. Lee, R. M. Kamens, *Science* **298**, 814 (2002).
7. E. M. Knipping *et al.*, *Science* **288**, 301 (2000).
8. Q. Du, R. Superfine, E. Freysz, Y. R. Shen, *Phys. Rev. Lett.* **70**, 2313 (1993).
9. E. A. Raymond, T. L. Tarbuck, M. G. Brown, G. L. Richmond, *J. Phys. Chem. B* **107**, 546 (2003).
10. K. R. Wilson *et al.*, *J. Phys. Chem. B* **105**, 3346 (2001).
11. K. R. Wilson *et al.*, *J. Chem. Phys.* **117**, 7738 (2002).
12. K. R. Wilson *et al.*, *J. Phys. Cond. Matter* **14**, L221 (2002).
13. R. Car, M. Parrinello, *Phys. Rev. Lett.* **55**, 2471 (1985).
14. D. Marx, J. Hutter, in *Modern Methods and Algorithms of Quantum Chemistry Proceedings*, J. Grotendorst, Ed. (John von Neumann Institute for Computing, Forschungszentrum Julich, Germany, ed. 2, 2000), NIC series, vol. 3, pp. 329–477.
15. J. Hutter *et al.*, CPMD v. 3.6.5 (MPI fur Festkorperforschung and IBM Zurich Research Laboratory, Rueschlikon, Switzerland, 1999).
16. G. Lippert, J. Hutter, M. Parrinello, *Mol. Phys.* **92**, 477 (1997).
17. M. A. Wilson, A. Pohorille, L. R. Pratt, *J. Phys. Chem.* **91**, 4873 (1987).
18. P. Vassilev, C. Hartnig, M. T. M. Koper, F. Frechard, R. A. van Santen, *J. Chem. Phys.* **115**, 9815 (2001).
19. Materials and Methods are available as supporting online material on *Science* Online.
20. Y. Harpaz, M. Gerstein, C. Chothia, *Structure* **2**, 641 (1994).
21. M. Gerstein, J. Tsai, M. Levitt, *J. Mol. Biol.* **249**, 955 (1995).
22. P. L. Silvestrelli, M. Parrinello, *Phys. Rev. Lett.* **82**, 3308 (1999).
23. P. L. Silvestrelli, M. Bernasconi, M. Parrinello, *Chem. Phys. Lett.* **277**, 478 (1997).
24. I. Benjamin, *Phys. Rev. Lett.* **73**, 2083 (1994).
25. A. Luzar, D. Chandler, *Nature* **379**, 55 (1996).
26. A. Luzar, D. Chandler, *Phys. Rev. Lett.* **76**, 928 (1996).
27. S. Myneni *et al.*, *J. Phys. Cond. Matter* **14**, L213 (2002).
28. K. Modig, B. G. Pfrommer, B. Halle, *Phys. Rev. Lett.* **90**, 075502 (2003).
29. M. Sprik, J. Hutter, M. Parrinello, *J. Chem. Phys.* **105**, 1142 (1996).
30. P. Hunt, M. Sprik, R. Vuilleumier, *Chem. Phys. Lett.* **376**, 68 (2003).
31. G. Berghold, C. J. Mundy, A. H. Romero, J. Hutter, M. Parrinello, *Phys. Rev. B* **61**, 10040 (2000).

32. This work was performed under the auspices of the U.S. DOE by University of California LLNL under contract W-7405-Eng-48. We would like to thank M. Parrinello, M. L. Klein, R. Saykally, J. Hutter, D. J. Tobias, J. I. Siepmann, K. R. Wilson, and the CP2K/CPMD Mannschaft for scientific guidance. Special thanks to J. VandeVondele, F. Mohamed, and M. Krack for help with the QUICKSTEP program. We acknowledge the Livermore Computing staff, C. Westbrook, and A. Kubota at LLNL.

Supporting Online Material

www.sciencemag.org/cgi/content/full/303/5658/658/DC1
Materials and Methods
SOM Text
Fig. S1
References

21 October 2003; accepted 2 December 2003